Preprint
UCRL-JC-138436

Dipole Septum Magnet in the Fast Kicker System for Multi-Axis Advanced Radiography

L. Wang, S.M. Lund, B.R. Poole

This article was submitted to
XX International Linac Conference, Monterey, CA
August 21-25, 2000

August 10, 2000

U.S. Department of Energy
Lawrence
Livermore
National
Laboratory

DIPOLE SEPTUM MAGNET IN THE FAST KICKER SYSTEM FOR MULTI-AXIS ADVANCED RADIOGRAPHY*

L. Wang, S. M. Lund, B. R. Poole, LLNL, Livermore, CA94550, USA

Abstract

Here we present designs for a static septum magnet with two adjacent apertures where ideally one aperture has a uniform dipole field and the other zero field. Two designs are considered. One is a true septum magnet with a thin layer of coils and materials separating the dipole field region from the null field region. During the beam switching process, the intense electron beam will spray across this material septum leading to concerns on beam control, vacuum quality, radiation damage, etc. due to the lost particles. Therefore, another configuration without a material septum is also considered. With this configuration it is more difficult to achieve high field quality near the transition region. Shaped shims are designed to limit the degradation of beam quality (emittance growth). Simulations are performed to obtain the magnetic field profile in both designs. A PIC simulation is used to transport a beam slice consisting of several thousand particles through the magnet to estimate emittance growth in the magnet due to the field non-uniformity.

1 INTRODUCTION

Linear induction accelerator based x-ray technology can provide time-resolved, 3-D radiography capabilities for a hydrodynamic event. A kicker system, which includes a stripline dipole kicker and a dipole septum magnet, is a key component of this technology [1]. The kicker system cleaves a series of intense electron beam micropulses, and steers the beam into separate beam transport lines to achieve multiple lines of sight. The first part of this fast kicker system is a high current stripline dipole kicker that is only capable of imparting a small angular bend to the beam centroid. This is followed by a static field dipole septum magnet that increases the angular separation of the centroids and steers them into separate transport lines.

The ideal "box" geometry of the septum magnet for our application is shown in Figure 1. There are two adjacent apertures where ideally one aperture has a uniform dipole magnetic field and the other zero field, separated by a thin septum in the field transition region. The two beams emerging from the kicker are incident on the magnet a radial distance d from the centerline and are further separated from each other by the dipole field as the beams traverse the axial length ℓ of the magnet. Given the beam energy, and the incident and exiting angles of the beam at the dipole septum magnet, the magnetic field needed to provide the desired bend can be calculated. Assuming the effect of the fringe field is neglected, the required dipole magnetic field B is related to the beam energy E_b and the incident and exiting beam angles θ_i and θ_f by

$$B\ell = \frac{mc}{e}\sqrt{\left(\frac{E_b}{mc^2}\right)^2 + 2\left(\frac{E_b}{mc^2}\right)}\left[\sin\theta_f - \sin\theta_i\right]. \qquad (1)$$

where m and e are the mass and charge of an electron, and c is the speed of light in vacuum. On traversing the magnet, the beam centroids will move radially a distance

$$\Delta = \ell\frac{\left[\cos\theta_i - \cos\theta_f\right]}{\left[\sin\theta_f - \sin\theta_i\right]}. \qquad (2)$$

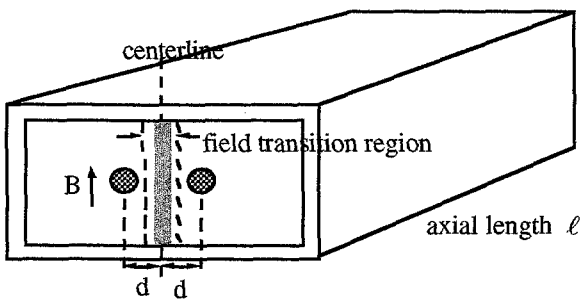

Fig. 1: Ideal box geometry of the dipole septum magnet.

2 SEPTUM MAGNET DESIGN

The parameters for the magnet design are an axial length $\ell = 50\,\text{cm}$, incident and exiting beam angles of $\theta_i = 1\,\text{deg}$ and $\theta_f = 22.5\,\text{deg}$, resulting in a bending field of $B \approx 500\,\text{Gauss}$ for the beam energy of $E_b \approx 20\,\text{MeV}$. The incident beam radius (r_b) and centroid separation ($2d$) at the septum magnet are about 0.7 cm and 5.6 cm, respectively. The beam centroid will exit the magnet a horizontal distance of $\Delta \sim 10.4\,\text{cm}$.

Two designs are considered. One is a true septum magnet with a thin layer of coils and materials separating the dipole field region from the null field region. Figure 2 shows the 2-D geometry of this septum magnet. The beam goes through the aperture ($2h$) of 10 cm. The

* The work was performed under the auspices of the U. S. Department of Energy by University of California Lawrence Livermore National Laboratory under contract No. W-7405-Eng-48

operational magnetic field in the gap is about 500 Gauss. The amp-turns of each coil in the simulations is $NI \approx Bh/\mu_0 \sim 1990$ amp-turns where h is the half gap, μ_0 the free space permittivity, and N the number of turns of the coil.

Figure 2: Geometry of a dipole septum magnet with a thin layer of coil separating dipole and null field regions.

During the beam switching process, the intense electron beam will spray across this material septum leading to concerns on beam control, vacuum quality, radiation damage, etc. due to the lost particles. Therefore, another configuration without a material septum is also considered. The schematic of the second design is shown in Figure 3. It is essentially two "C" type dipole magnets brought into close radial proximity. With this configuration it is more difficult to achieve high field quality near the transition region. The rapidity of the transition between the dipole field and null field regions depends critically on h/d, the ratio of magnet half-gap h relative to the incident centroid displacement d. The ratio d/r_b, where r_b is the beam radius, must also be sufficiently large such that the incident beam does not enter the field transition region. Achievable d is limited by the fast kicker technology and the maximum fast kicker to septum magnet drift distance. Thus we would like h to be as small as possible in order to obtain good field quality in the field transition region. However, h has to be large enough to allow easier beam tuning through the magnet aperture. To enhance field linearity and limit the degradation of beam quality (emittance growth), shims are designed and employed near the field transition region.

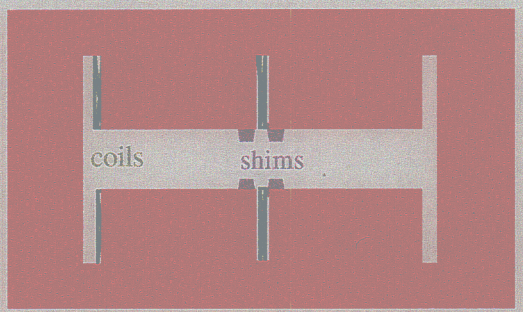

Figure 3: Schematic of the second dipole septum magnet design which does not have a material septum between the dipole field region and the null field region.

3 MAGNETIC FIELD SIMULATION

The magnetic field in the dipole septum magnet was simulated using the 2-D magnetostatic Poisson code. Only a half of the symmetric structure was simulated. There is no iron saturation for the full possible coil excitation. Figure 4 displays the field contours for the dipole septum magnet which has a thin layer of coils in the middle. There is a perfect dipole field on the left side as indicated by the straight field lines.

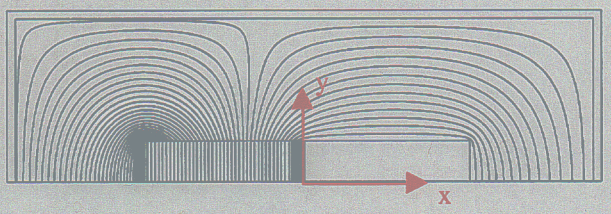

Figure 4: Simulated field lines in the half aperture of the dipole septum magnet with a thin layer of coils in the middle.

The vertical magnetic field on the midplane (y = 0) of the magnet as a function of x is plotted in Figure 5. The figure shows that the magnetic field on the left side is about 500 Gauss as we have predicted. Magnetic field goes from the maximum value to a small number in a short distance. The electron beam entering the dipole field side of the magnet experiences a uniform field when it traverses the magnet. The simulation result also shows that there is a small leakage field in the null field region. With the use of μ–metal sheet enclosure (shown in Figure 6) , the magnitude of the magnetic field is reduced to less than 0.2 Gauss.

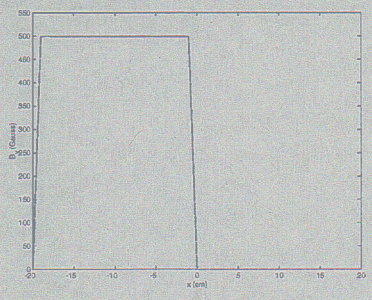

Figure 5: Vertical magnetic field on the midplane of the septum magnet (with a material septum).

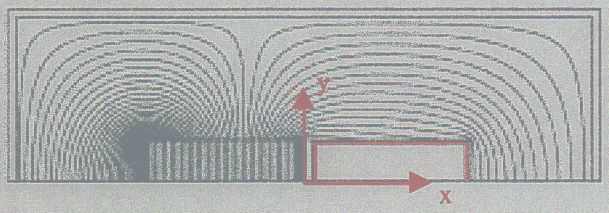

Figure 6: Simulated field lines in the half aperture of the dipole septum magnet. The use of μ–metal enclosure helps reduce the leakage field in the null field region.

The simulated field contours for the magnet without a material septum separating the dipole field region from the null field region is shown in Figure 7. Blue semicircles in the figure illustrate the positions of the incident electron beams emerging from the kicker. The curved field lines near the field transition region indicate non-uniform fields. With this configuration, both beams experience non-uniform field which can lead to emittance growth. Compared to the magnet with a material septum, it's more difficult to achieve high field quality near the transition region with this design.

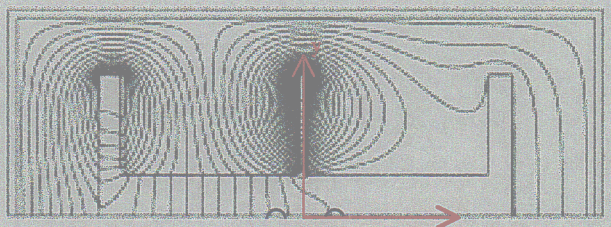

Figure 7: Simulated field lines in the half aperture of the dipole septum magnet (without a material septum).

To enhance field linearity near the transition region, shims of trapezoidal shape are designed. From Figure 8, we can see that the field lines are straighter near the incident beam position in the dipole field region. Fields in the transition region are more uniform with the use of shims. In addition, μ–metal sheet enclosure is also utilized to reduce in the leakage field in the null field region. The effect of the shim is further illustrated in Figure 9, where the vertical magnetic field on the midplane (y=0) of the septum magnet is plotted. The solid curve represents the magnetic field for the case where no shim nor μ–metal sheet enclosure is used. It takes more than 10 cm for the magnetic field to go from the maximum value to a small number. The leakage field in the null field region is quite high. The field at the edge of the incident beam in the null field side is about 80 Gauss. With the use of the μ–metal sheet enclosure (dashed curve), the field drops to less than 0.1 Gauss at that location. The third curve represents the case where both shims and μ–metal sheet enclosure are utilized. The curve shows that the shim reduces the undesirable variation in field at the beam edge and centroid for the beam in the dipole field region. The electron beam entering the dipole field side of the magnet experiences a more uniform field when it traverses the magnet.

4 EMITTANCE CALCULATION

To determine beam quality for the various magnet designs, a PIC code is utilized to examine the emittance growth in the magnet [2]. The 20 MeV beam slice is transported through the magnetic field region using the 2-D field map for the structure. The results show that

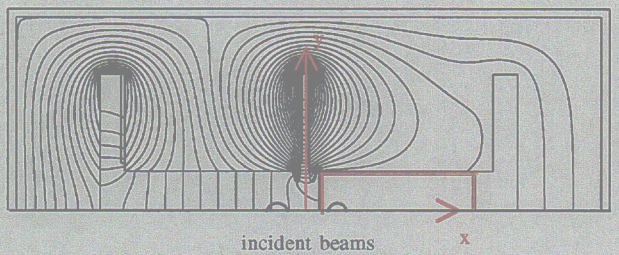

Figure 8: Simulated field lines in the half aperture of the dipole septum magnet (without material septum). Shims are used to make fields more uniform in transition region.

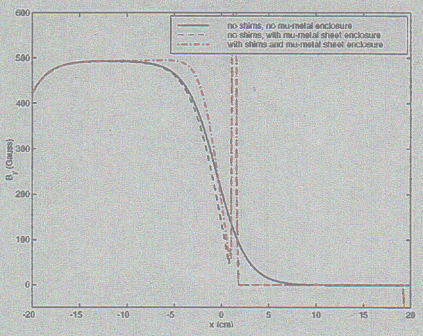

Figure 9: Vertical magnetic field on the midplane of the septum magnet (without a material septum).

there is no emittance growth when the electron beams go through the dipole septum magnet with a thin layer of coils separating the dipole field region from the null field region. For the design with no septum material in the middle, there is no emittance growth when the beam traverse through the null field region and 6% emittance growth when the beam goes through the dipole field region. The emittance growth can be further reduced by designing the shim in greater detail.

5 CONCLUSION

Two designs of a dipole septum magnet for the use in multi-axis advanced radiography are presented. One design avoided the use of a material septum. To improve the field quality near the transition region in this design, shaped shims are designed. Simulations are performed to estimate the emittance growth in the magnet for both designs.

6 ACKNOWLEDGEMENT

The authors wish to thank G. Caporaso, Y.-J. Chen, and G. Westenskow for helpful technical suggestions.

REFERENCES

[1] Y.J. Chen, et. al., "Precision Fast Kicker for Kiloampere Electron Beams", PAC 99, New York, March 29- April 2, 1999.

[2] B.R. Poole, et. al., "Analysis and Modeling of a Stripline Beam Kicker and Septum", LINAC 98, Chicago, IL, August 23-28, 1998.

Matlab Curve Fit to Gaussian Integral